The central Kenya peralkaline province: Insights into the evolution of peralkaline salic magmas.

Ray Macdonald, Bruno Scaillet

The central Kenya peralkaline province: Insights into the evolution of peralkaline salic magmas

R. Macdonald[a,] and B. Scaillet[b]

[a]Environment Centre, Lancaster University, Lancaster LA1 4YQ, UK
[b]ISTO-CNRS, 1a rue de la Férollerie, 45071 Orléans cedex 2, France

Abstract

The central Kenya peralkaline province comprises five young (< 1 Ma) volcanic complexes dominated by peralkaline trachytes and rhyolites. The geological and geochemical evolution of each complex is described and issues related to the development of peralkalinity in salic magmas are highlighted. The peralkaline trachytes may have formed by fractionation of basaltic magma via metaluminous trachyte and in turn generated pantellerite by the same mechanism. Comenditic rhyolites are thought to have formed by volatile-induced crustal anatexis and may themselves have been parental to pantelleritic melts by crystal fractionation. The rhyolites record very low temperatures of equilibration (≤ 700 °C) at low fO_2 (≤ FMQ). The development of compositional zonation within the magma reservoirs has been ubiquitous, involving up to tens of cubic km of magma at timescales of 10^3–10^4 years. Magma mixing has also been commonplace, sometimes between adjacent centres. Isotopic evidence relating to rates and timescales of pre-eruptive residence times and crystal fractionation processes is summarized.

Keywords: Kenya; Petrogenesis; Peralkaline magmas

1. Introduction

In the central Kenya Rift Valley, a unique petrographic province comprises five Quaternary–Recent, peralkaline salic volcanic complexes. Three are trachytic caldera volcanoes (Menengai, Longonot and Suswa) and two are rhyolitic complexes (Eburru, Olkaria; Fig. 1). The trachytes range in composition from metaluminous to peralkaline and from silica-oversaturated to silica-undersaturated, and the rhyolites from comendite to pantellerite. Adjacent complexes can be less than 10 km apart but chemical features indicate that all five complexes are distinct and derived from separate magmatic systems. Fig. 2 shows alkali–silica relationships in the complexes and in three, basalt-dominated, minor centres which are geographically associated with them; the Elmentaita centre lies just to the north of Eburru, the Ndabibi centre between Eburru and Olkaria, and the Akira centre between Olkaria and Suswa.

Although problems of detail remain, the stratigraphical relationships within and between complexes are well known. The region has thus provided an excellent opportunity to place the high-level stages of peralkaline magmatism into a time–volume compositional context and to describe in detail the structural and geochemical evolution of the centres. We now have a fair understanding of the differentiation processes operating within the trachytic and rhyolitic systems. Progress has also been made in establishing rates and timescales of magmatic and structural evolution. Importantly for peralkaline rocks, given the chemical modifications which normally accompany crystallization and secondary hydration, all the complexes contain pristine glassy material, allowing us to describe liquid lines of descent with some confidence.

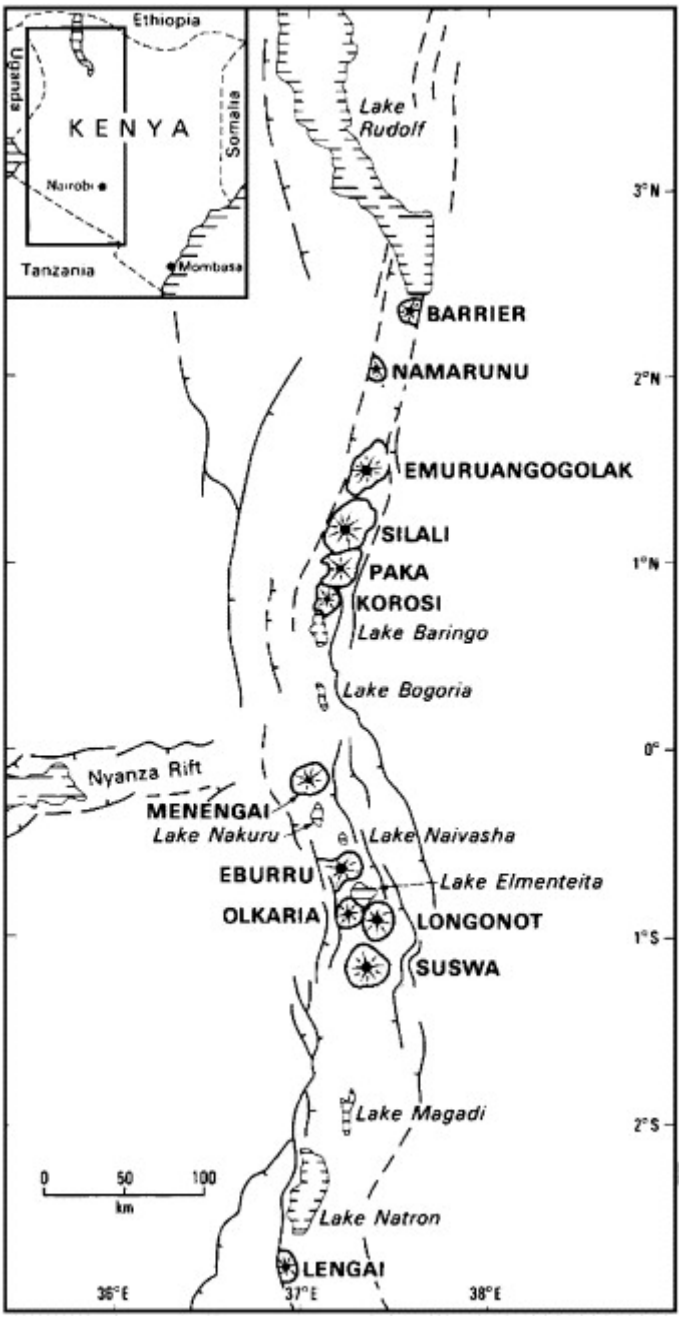

Fig. 1. Location of Recent peralkaline trachyte caldera volcanoes (Menengai, Longonot and Suswa) and peralkaline rhyolite complexes (Eburru, Olkaria) in the south-central Kenya rift. Also shown are Recent volcanoes in the northern rift sector. From Clarke et al. (1990).

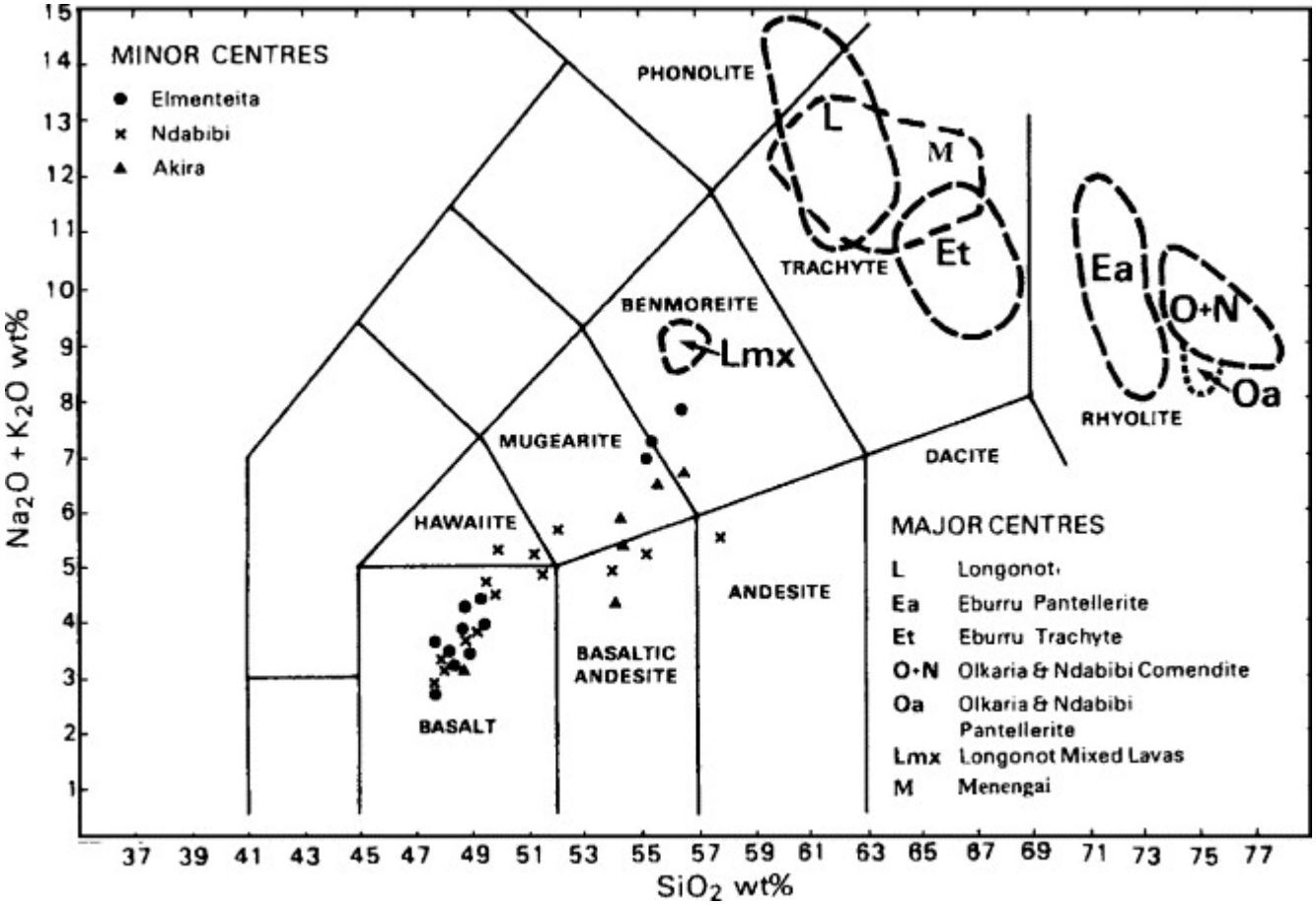

Fig. 2. Alkali–silica plot showing the compositional range in each centre and in three minor centres geographically associated with them. Modified from Clarke et al. (1990). Suswa has been omitted due to a lack of geochemical data.

The rocks also provide an excellent, and as yet underutilised, opportunity to describe in great detail melt–crystal relationships during magmatic evolution, including the possibility of tracing changing trace element partitioning patterns as melt composition, pressure and temperature change.

In this review, we assess how the study of the central Kenyan complexes has contributed to our understanding of the origin and evolution of peralkaline magmatic suites. We also indicate outstanding problems requiring further work.

2. Regional setting

The central rift peralkaline province coincides with an area of crustal upwarping known as the Kenya Dome, the apical region of which lies near Lake Nakuru (Fig. 1). The Dome is associated with only minor (~1 km) amounts of uplift and is apparently in isostatic equilibrium, supported by the loading of anomalous mantle within the underlying lithosphere (Smith, 1994).

Crustal thickness beneath the Kenya Dome is 30–35 km (Mechie et al., 1997). The upper crust (~12 km thick) mainly comprises quartzo-feldspathic gneisses and schists, whereas the middle crust (~12–14 km) consists of more mafic, hornblende-rich metamorphic rocks, probably intruded by mafic rocks. The lower crust (~9 km) may be a mix of high-grade

metamorphics and underplating mafic and ultramafic material (Mooney and Christensen, 1994 and Mechie et al., 1997). A −190 mGal gravity high centred on the rift axis and coincident with the central complexes has been modelled by Swain (1992) as resulting from pervasive dyke injection in the central 40 km of the rift, in which 22–26% of the present-day crust, down to a depth of 22 km, consists of intruded material. Swain (1992) envisages each of the central volcanoes as representing a nexus, where the regional dyke swarm has developed a high-level reservoir. We shall see that this structure has influenced the petrological development of the volcanic complexes.

We have relatively little information on the depths at which the magma chambers underlying the salic complexes exist. Swain (1992) modelled a gravity high directly under the Menengai caldera as representing a mafic intrusion (density 2900 kg m^{-3}) in the uppermost 5 km of the crust. The rift floor in the province is cut by swarms of closely spaced normal faults which virtually die out on the shields of the salic centres. Following Mahood (1984), Macdonald (1987) interpreted this to indicate the presence at shallow depths of partially molten zones which cannot support brittle fracture. Scaillet and Macdonald (2001) experimentally reproduced the phenocryst crystallization sequence in peralkaline rhyolites of the Olkaria complex in the pressure range 50–150 MPa, i.e. < 5 km depth. It is reasonable to suppose, therefore, that the high-level reservoirs beneath the complexes lie at < 10 km depth.

3. Menengai Volcano

The evolution of the trachytic caldera volcano Menengai (lat. 0°12′S, long. 36°04′E) is recorded in the complex compositional variations with time, summarized on an FeO–Zr plot (Fig. 3); details are provided by Leat et al. (1984) and Macdonald et al. (1994). Activity started at 180 ka with the growth of a lava shield and lasted ~150 ka, forming a volume of ~ 30 km^3 (Leat, 1984). The dominant eruptive products of the shield phase were peralkaline trachytes, showing relatively little compositional variation (× 1.25 for major elements). Leat et al. (1984) recognised two compositional end-members: one higher in Ca, Fe, Sr, Y and Zn and the REE, the other with slight enrichment in Al, K, Zr, Nb and Th. With time, the Y-related end-member tended to become dominant, although there were frequent reversals toward the lower Y-type. Leat et al. (1984) interpreted this to indicate periodic addition of new magma batches to the growing magma system (Fig. 3, stage 1).

A series of pantelleritic trachyte tuffs probably represent late pre-caldera activity but their exact age relationships to the shield lavas are not known. Chemical variation in the tuffs is similar to that in the lavas but, on average, the tuffs are more evolved, in the sense of having higher abundances of the incompatible trace elements and lower concentrations of Mg, Al, P and Sr. Leat et al. (1984) argued that a low-density, volatile-rich cap became separated from the main lava-producing zone by a stable interface (Fig. 3, stage 2A). Chemical variations within some individual tuff units indicate that some were erupted from a compositionally zoned reservoir, a process that was to be continuously repeated as Menengai evolved. In late pre-caldera times, trachyte magma was able to penetrate into the cap zone, resulting in the formation of mixed magmas (Fig. 3, stage 2B).

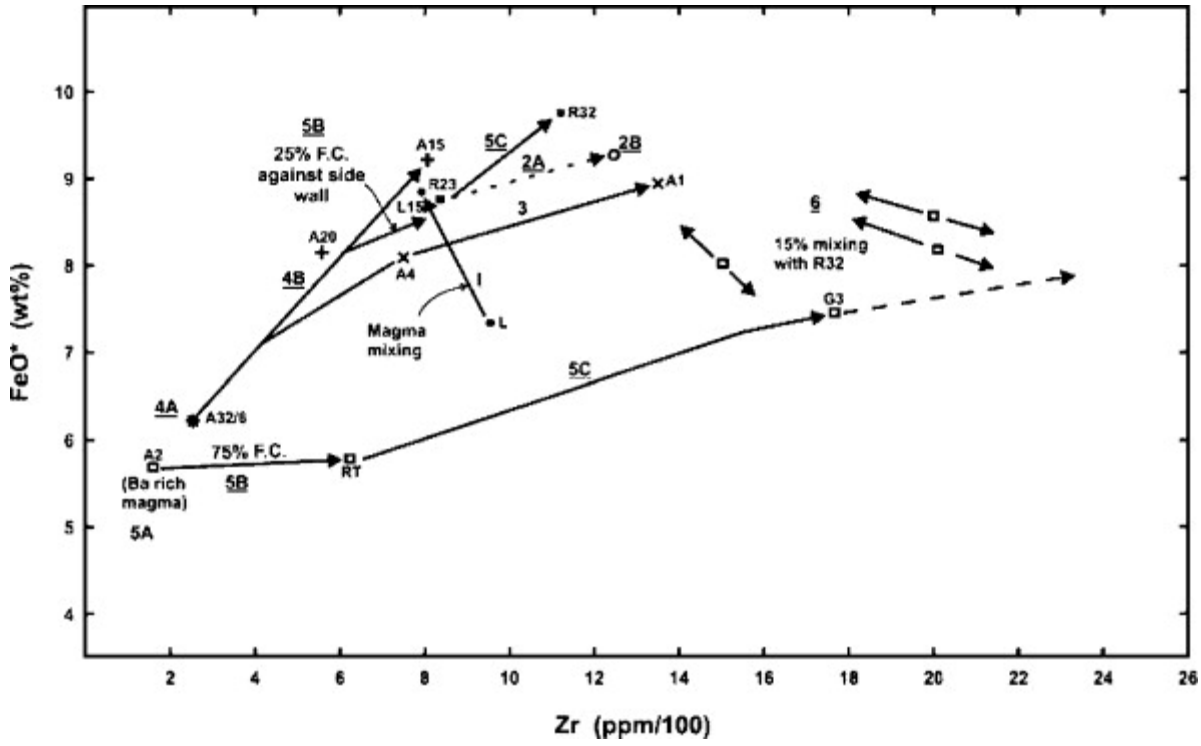

Fig. 3. FeO*–Zr plot summarizing the geochemical evolution of Menengai. Specimen numbers (e.g. A20, A2) refer to analyses given in Leat et al. (1984). Redrawn from Leat et al. (1984).

Growth of the lava shield was truncated, at ~29 ka, by a period of caldera collapse, accompanied by the eruption of an ash flow tuff, preceded by pumice falls. The ash flow tuff had a volume of 20 km^3 and was erupted as a single flow unit (Leat, 1984). It was compositionally zoned; the earliest erupted products were pantelleritic trachytes, the last comenditic trachytes, and there is continuous chemical variation throughout the fall-ash flow sequence, which is particularly strong in the fall deposits and early part of the ash flow tuff. Leat et al. (1984) inferred that the sequence was erupted from a compositionally zoned magma chamber which showed strong upward enrichment in Fe, Mn and the incompatible trace elements (ITE) and probably also Na and the halogens, and roofward depletion in Al, Mg, Ca, K, Ti, P, Ba and Sc (Fig. 3, stage 3). Enrichment factors of up to 5 are observed for some elements, e.g. Nb, Ta, Zr, Hf, Ta and Th. Leat et al. (1984) ascribed compositional variations within the sequence to liquid state differentiation and minor crystal fractionation. Later work on the products of a second caldera collapse (Macdonald et al., 1994) make it much more likely that crystal fractionation was the major differentiation mechanism (see below).

Following eruption of the ash flow, volatiles were lost to the atmosphere via fractures in the cauldron block. The Fe-rich, cooler magma in the upper part of the chamber now had a density higher than the underlying, lower Fe-trachyte. This promoted convective overturn and the production of a homogenised magma (Fig. 3, stage 4A; Fig. 4A).

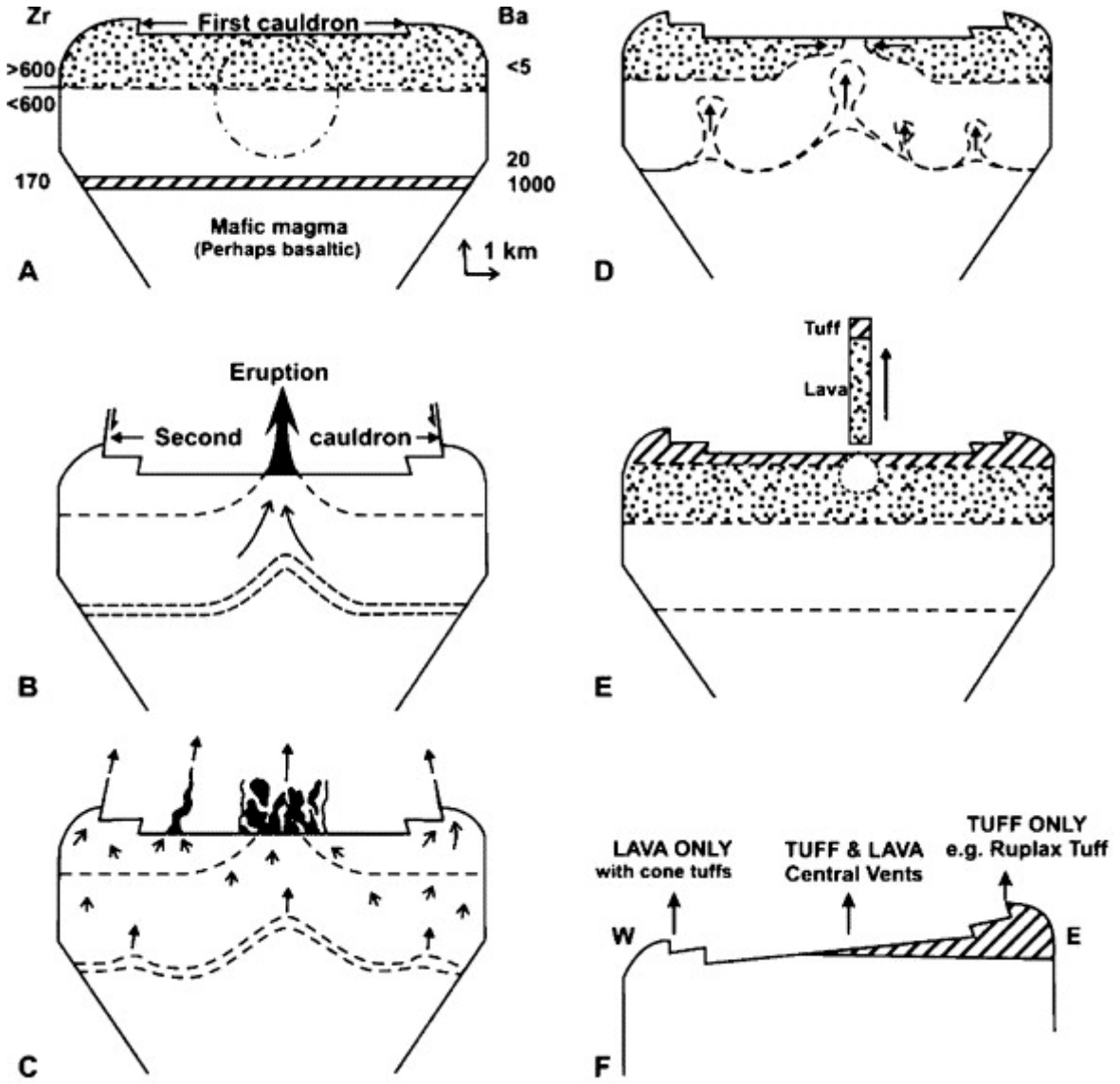

Fig. 4. Schematic representation of the evolution of the Menengai magma chamber from before eruption of the second ash flow tuff to the present day. From Leat et al. (1984). (A) Speculative view of the chamber prior to eruption of the second ash flow. The dot-dash area represents the volume of magma to be erupted as the ash flow. (B) The displacement of the previously horizontal isochemical zones after the eruption is shown. (C) Escape of volatiles after caldera collapse. Smaller arrows show direction of volatile migration; heavier arrows indicate the buoyant rise of a Ba-rich layer. (D) Ba-rich layer assumed to rise as diapirs towards the chamber roof. (E) Ba-rich layer (diagonal lines) forms the roof zone, where it evolves to the tuff-forming magma. Magma formerly at the roof forms the lava-producing zone (stippled). The dotted line encloses the volume of magma typically erupted in a single post-caldera eruption. (F) A slightly more realistic version of (E), showing the westerly tilt of the chamber roof and the different combinations of eruptive products across the caldera

A second period of collapse occurred at ~8 ka, with the formation of a 12 × 8 km caldera associated with the eruption of a second fall-ash flow tuff sequence (Fig. 3, stage 4B; Fig. 4B). The tuff represented some 30 km^3 of magma and had an outflow sheet aspect ratio of 1:4000. The stratigraphy of the fall-ash flow tuff deposits was described by Leat, 1984 and Leat, 1985 and Macdonald et al. (1994), along with details of thickness, degree of welding, clast content, and distribution. Like the first ash flow tuff, the tuff is inferred to have been erupted from a compositionally zoned magma chamber, with strong roofward enrichment in Fe, Mn, Na and the ITE and depletion in Al, Mg, Ca, K, Ti, P and Ba, corresponding to

pantelleritic trachyte at the top, grading down through comenditic trachyte to more primitive, Ba-rich, trachyte. The maximum observed enrichment factor is × 4 for Zr, slightly less than in the first ash flow tuff (Leat et al., 1984 and Macdonald et al., 1994). $^{87}Sr/^{86}Sr$ becomes less radiogenic (from 0.7062 to 0.7048) and $^{143}Nd/^{144}Nd$ more radiogenic (ε_{Nd} from 0 to − 2) upwards, suggesting that the chamber may also have been zoned isotopically (Macdonald et al., 1994).

As eruption proceeded, a range of compositions was progressively tapped; zonation in the chamber is inferred to have been continuous. Variable matrix glass compositions within individual specimens and unusually sodic cores of feldspar phenocrysts in some rocks were thought by Macdonald et al. (1994) to result from mixing of melts from more than one compositional layer during magma withdrawal.

Leat et al. (1984) argued that compositional variation within the second fall-ash flow tuff sequence resulted from liquid state differentiation, probably involving volatile transfer and thermodiffusion, and minor crystal fractionation. Using a more complete set of crystal/melt partition coefficients, Macdonald et al. (1994) showed that the zonation resulted from up to 75% fractional crystallization of an alkali feldspar–olivine–clinopyroxene–titanomagnetite–apatite assemblage from the least evolved trachytes, accompanied by minor assimilation of wall rocks, especially in the deeper (hotter?) parts of the chamber.

Some samples of the ash flow tuff from the eastern caldera wall are unusually rich in Ba (up to 120 ppm; Macdonald et al., 1994) and seem to have entrained 7–20% of an underlying Ba-rich layer, which was to make a reappearance during post-caldera activity.

Collapse of the second caldera was followed by convective overturn within the chamber and the rise to the roof zone of a Ba-rich magma, where it formed a layer overlying, and separated by a stable density interface from, the low-temperature, Fe-rich magma formerly at the roof (Fig. 3, stage 5A; Fig. 4D). The upper layer generated tuffs (representing ~2 km^3 of magma), the lower layer lavas (~23 km^3; Fig. 4E, F). In the latter, 25% of crystallization of syenite took place across the side walls. Crystallization was more extensive in the tuff-forming layer, some 75%, and the tuffs include more evolved compositions than the lavas (Fig. 3; stages 5B and C). Both layers developed compositional zonation, comparable to that shown by the earlier ash flow tuffs. Some mixing of the layers may have occurred in very recent times (Fig. 3, stage 6). Although for convenience Leat et al. (1984) chose to refer to all Menengai products as trachytic, the more evolved members of the post-caldera activity are, strictly speaking, pantelleritic rhyolites.

An important general observation from Menengai is that extreme compositional zonation, with observed enrichment factors > 5 for some elements in some units, were developed repeatedly through tens of cubic kilometres of magma in times of 10^2–10^4 years. These high rates were ascribed by Leat et al. (1984) to the high-halogen, high-Fe, relatively low viscosity nature of the melts.

4. Eburru volcanic complex

The complex (0°38′S, 36°15′E) covers an area of 470 km^2 and has the form of a 23 km ridge projecting from the western rift margin (Fig. 1). There have been four separate stages of evolution (Clarke et al., 1990). The precise age of the initiation of the activity is not known

but is < 0.45 Ma (Clarke et al., 1990), whilst the youngest activity is probably only hundreds of years old.

Building of a volcano pile at Western Eburru. The products of this stage are poorly exposed due to blanketing by later pyroclastics but were apparently dominated by welded and unwelded pantelleritic pyroclastics.

Eruption of the Waterloo Ridge fissure zone. Pyroclastic eruptions along an N–S elongate fracture generated pumice falls and flows of pantellerite composition, both commonly welded.

Building of a volcanic pile at Eastern Eburru. As for stage 1, the products of this activity are largely blanketed by younger deposits but seem to have been mainly pantelleritic and pantelleritic trachyte pumice and ash falls. Later activity was dominated by lava flows and (often welded) cone pyroclastics of pantelleritic trachyte.

Axial activity at Eastern Eburru. A series of pantelleritic lava flows and pyroclastic cones is associated with a notable N–S fracture zone running from the Olkaria Complex in the south to the Elmenteita basalt field in the north. Some of the flows show evidence of mixing of pantellerite and pantelleritic trachyte magmas.

Lithologically, rocks of the Eburru Complex have been divided into the Eburru Trachyte, which includes pantelleritic trachytes and pantellerites using the classification scheme of Macdonald (1974), and the Eburru Pantellerite. Mixing between rhyolitic and trachytic magmas is occasionally observed. Judging from $FeO^{\square}$–Al_2O_3 relationships (Fig. 5), the two lithologies are not directly related to each other but have evolved along parallel liquid lines of descent. The Eburru Trachyte is compositionally similar to the post-caldera pantelleritic trachyte–pantellerite suite at Menengai. Petrographic information on Eburru rocks can be found in Clarke et al. (1990) and Ren et al. (2006-this volume). Ren et al. (2006-this volume) report temperatures estimated using the QUILF methodology of 756–719 °C for the trachytes and 708–700 °C for the pantellerites and low fO_2 (ΔFMQ + 0.5 to − 1.6) for both rock types.

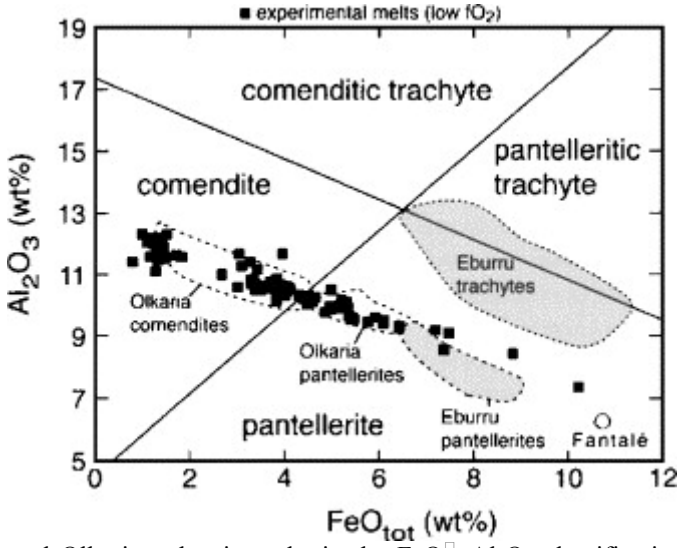

Fig. 5. Fields of Eburru and Olkaria volcanic rocks in the $FeO^{\square}$–Al_2O_3 classification diagram of Macdonald (1974). Also shown are the compositions of experimental glasses (melts) obtained by crystallization of natural Olkaria obsidians. Note that the Olkaria comendites and pantellerites and the Eburru pantellerites form similar liquid lines of descent, whereas the Eburru trachytes apparently form a different lineage. From Scaillet and Macdonald (2003).

Clarke et al. (1990) noted that between stages 2 and 3, there was a change to rocks with somewhat lower ITE abundances and slightly higher Zr/Nb ratios, which they equate to the higher pyroclastic content of the earlier formations. Despite being more peralkaline, the Eburru rocks have lower maximum ITE abundances (with the exception of Zr) than the comendites of the neighbouring Greater Olkaria Volcanic Complex (GOVC), perhaps indicating a less prolonged liquid line of descent, derivation from parental magmas poorer in ITE than those at Olkaria, or no/less involvement of an ITE-bearing vapour phase in their genesis. They also have lower LILE/HFSE ratios.

No petrogenetic study of the Eburru rocks has yet been published. However, Scaillet and Macdonald (2003) showed experimentally that strong fractionation of comenditic rhyolites from the Olkaria complex generated residual melts closely similar in major element terms to the Eburru pantellerites (Fig. 5). It may be, therefore, that the Eburru magmas were formed in similar manner.

Bailey and Macdonald (1975) used data from pantellerites and pantelleritic trachytes to show that Zr and Rb were linearly coordinated with F, and Y and Nb with Cl. They suggested that the metallic elements formed preferred complexes with either F or Cl and argued that the trace element patterns were controlled by a halogen-bearing vapour phase. These results will need to be revisited when a complete petrological study is available.

5. Greater Olkaria Volcanic Complex

The Greater Olkaria Volcanic Complex (GOVC; the Naivasha Complex of Macdonald et al., 1987) is a multicentred volcanic field some 240 km^2 in area and comprising at least 80 small centres. Comenditic lavas and pyroclastics dominate surface outcrops but trachyte and basalt–hawaiite lavas and pyroclastics have been minor products of the activity (Fig. 6). Minor basaltic centres also lie to the north (Ndabibi) and south (Akira) of the GOVC (Fig. 2).

The most recent history of the GOVC has been divided into six stages (Clarke et al., 1990). The earliest stage, of uncertain age, resulted in a pile of dominantly trachytic lava and pumice. This was followed by formation of a caldera, represented by welded pantellerites. Early post-caldera history (stage 3) saw the eruption of lavas and pyroclastics of comendite composition (the Lower Comendite member; > 9150 ± 110 BP). The Middle Comendite member (stage 4; < 9150, > 3280 BP) was commonly ring dome building but also involved thick surge deposits. There was a general resurgence during the fifth stage of the activity, the Upper Comendite member (> 3280 BP), which built short thick comendite flows. The final stage was centred on an N–S fissure, its most notable expression being a very thick comendite flow, dated at 180 ± 50 BP by ^{14}C.

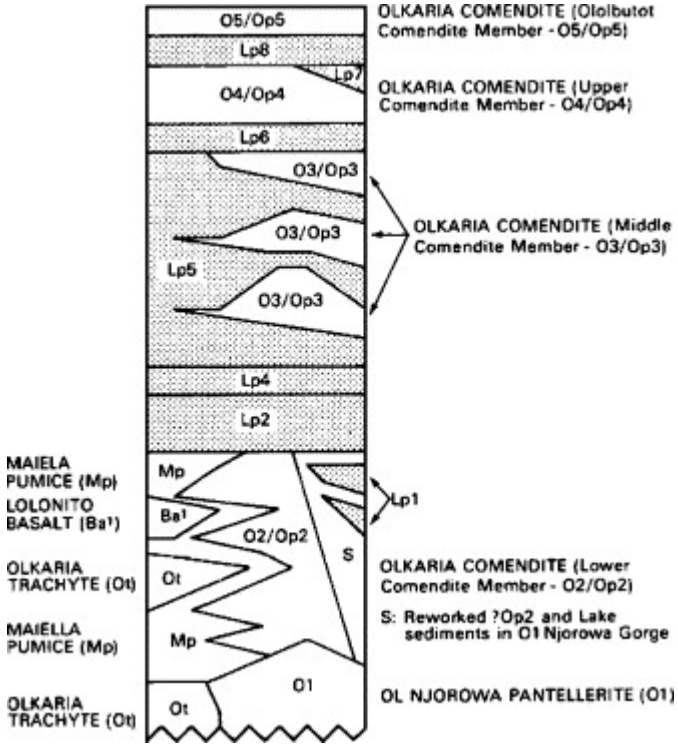

Fig. 6. Summary of Olkaria stratigraphy and its relationship to the neighbouring Longonot volcano. Lp numbers refer to Longonot stratigraphic units—see Fig. 8. From Clarke et al. (1990).

Groups of coalesced domes and flows form distinct topographic features across the complex. These groups also show compositional and mineralogical differences to adjacent groups and this led to the concept of discrete centres whose high-level magmatic systems have remained unconnected during evolution of the complex (Macdonald et al., 1987, Davies and Macdonald, 1987, Black et al., 1997 and Heumann and Davies, 2002).

In major element terms, the Olkaria comendites are typical of the lithology. Peralkalinity indices range from 1.01 to 1.4 and increasing peralkalinity is marked by increases in Na and Fe and decreases in Si, Al, Mg and Ca. The trace element characteristics are, however, distinctly unusual. There is extreme enrichment in certain ITE (e.g. Nb, 1000 ppm; Th, 250 ppm; Rb, 1000 ppm) and F (> 1 wt.%), and extreme depletion in Ba (< 5 ppm) and Sr (< 1 ppm).

Although Bailey (1974) and Bailey and Macdonald (1987) argued on geological and petrological grounds that the Olkaria comenditic magmas were relatively anhydrous, data from melt inclusions in quartz phenocrysts (Wilding et al., 1993) and experimental evidence (Scaillet and Macdonald, 2001) showed that the pre-eruptive magmas contained up to nearly 6 wt.% H_2O. The experiments also suggested that the comendite phenocryst assemblages crystallized at relatively low fO_2 (at or below FMQ), at very low temperatures (between 740 and 660 °C) and under near water-saturated conditions. Similarly low temperatures and fO_2 have been recorded from the Kane Springs Wash complex in Nevada (Novak and Mahood, 1986) and the Eburru complex (Ren et al., 2006-this volume); the temperatures are among the lowest recorded for peralkaline silicic rocks.

Lead isotope (Davies and Macdonald, 1987) and U-series disequilibria (Black et al., 1997 and Heumann and Davies, 2002) data showed that the Olkaria comendites have different isotopic

characteristics to basalts and hawaiites from the complex (Fig. 7). This, in tandem with the absence of intermediate compositions among the extrusives and with LILE/HFSE ratios which are unusually high for peralkaline rhyolites, were interpreted to mean that the comenditic magmas were generated by partial melting of crustal rocks in the presence of an alkali- and halogen-rich volatile phase (c.f. Macdonald et al., 1987). This left unexplained some critical aspects of their composition, in particular the extremely low Ba and Sr contents, which are almost impossible to generate during anatexis of normal crustal lithologies (Heumann and Davies, 2002). The problem was heightened through study of the wide range of magmatic inclusions which occur in the comendites. These range from hawaiite to trachyrhyolite and, with the extrusive basalts and trachytes, form a complete compositional spectrum from magnesian basalt to comendite (Marshall and Macdonald, 1998). We are currently involved in studies aimed at resolving the origin of the comendites.

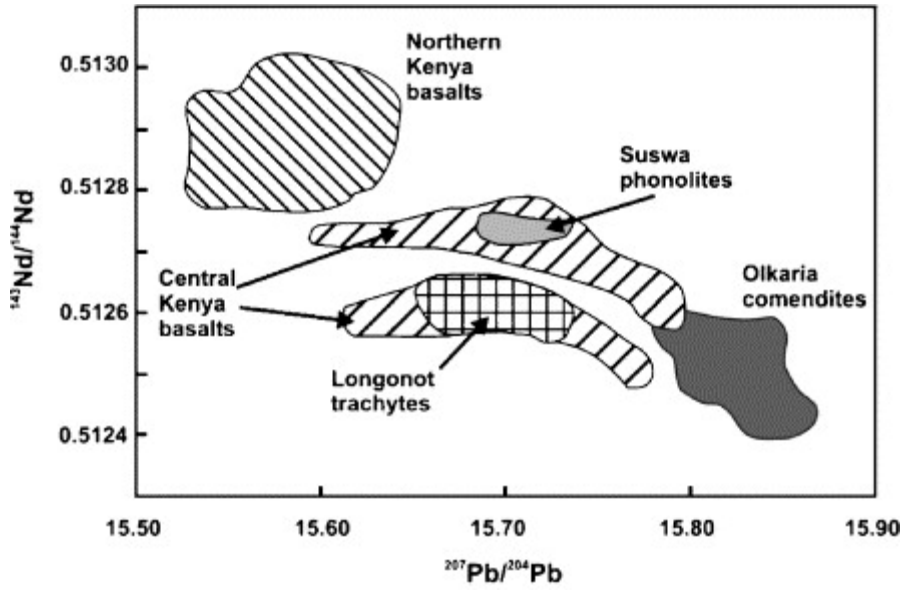

Fig. 7. Covariation of $^{143}Nd/^{144}Nd$ with $^{207}Pb/^{204}Pb$ in rocks from Suswa, Longonot and Olkaria. Note that whilst the Suswa and Longonot rocks overlap with the fields of basalts from central Kenya (including basalts from the Olkaria region, which plot in both "Central Kenya" fields), the Olkaria comendites occupy a separate field. Modified from Rogers et al. (2004).

Whatever the ultimate origin of the rhyolite magmas, it seems highly likely that compositional variation within them was controlled by fractional crystallization. Scaillet and Macdonald, 2001 and Scaillet and Macdonald, 2003 were able to reproduce the composition of the most from the least peralkaline comendites by extreme (~95–99 wt.%) crystallization of alkali feldspar–quartz-dominated assemblages.

An important result of the work of Scaillet and Macdonald (2003) was to identify one way to produce peralkaline liquids from (near-)metaluminous sources, by what they termed the clinopyroxene effect. As long as calcic pyroxene is stable, a marginally peralkaline rhyolite has little potential to increase the peralkalinity of residual liquids. When, however, fO_2 drops below NNO-1, clinopyroxene breaks down and the derivative melts are more peralkaline than coexisting feldspar. Further feldspar fractionation leads to increasingly peralkaline melts.

In a U–Th disequilibrium and Rb–Sr age study of comendites from the Gorge Farm Centre, Heumann and Davies (2002) showed that there was major chemical fractionation at 24 ± 1 ka,

some 16 ky before eruption. There was weaker evidence for an earlier event at 47 ± 0.2 ka. Using information from elsewhere in the complex and from Black et al. (1997), Heumann and Davies (2002) deduced that magma storage times at the GOVC have been around 22 ka, making the point that to keep such comparatively small magmatic reservoirs (estimated at 2–10 km^3) at near-liquidus conditions, as required by their aphyric/phenocryst poor nature, would need thermal support, perhaps from underlying basaltic magmas.

An important result of the experimental work of Scaillet and Macdonald, 2001 and Scaillet and Macdonald, 2003 was that protracted fractionation of the Olkaria comendites generated melt compositions indistinguishable, in major element composition, from the pantellerites of both Olkaria and Eburru (Fig. 5). This raises the possibility that the Eburru rocks were also ultimately derived by crustal anatexis and may have had a different origin from the Eburru Trachyte.

6. Longonot Volcano

The geology of the Longonot Volcano (0°55′S, 36°25′E) has been described by Scott (1980), Clarke et al. (1990) and Scott and Skilling (1999) and petrographical details were provided by Scott (1982), Scott and Bailey (1986), Clarke et al. (1990) and Rogers et al. (2004). The stratigraphy and structural events are summarized in Fig. 8. There are three distinct phases. The earliest phase, represented by the Olongonot lavas and pyroclastic deposits, lasted from 0.4 Ma to ca. 21,000 years BP and resulted in the construction of a composite trachyte cone, with a basal diameter of 25 km and a volume of ~280 km^3.

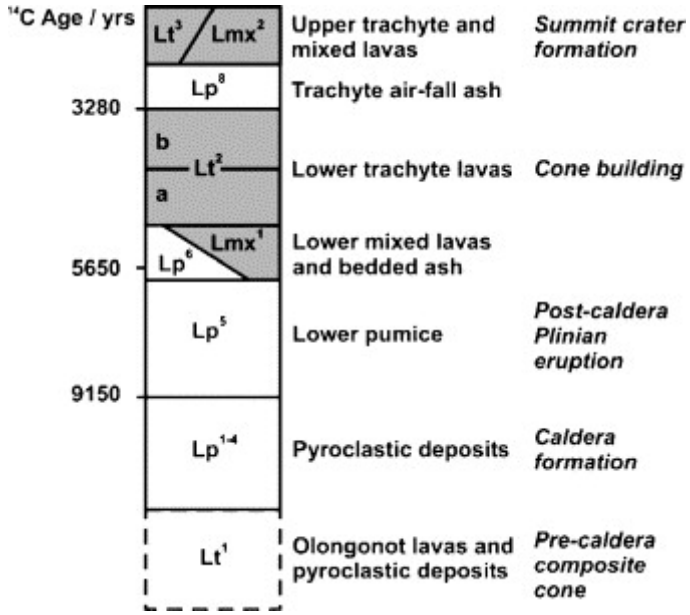

Fig. 8. Schematic stratigraphic column for the Longonot volcano. The shaded areas are the lava sequences shown in Fig. 9. Redrawn from Rogers et al. (2004).

Growth of the cone was terminated by the formation of a caldera some 7.5 km across and with a minimum volume of 26.5 km^3. Emplacement of at least 5 ignimbrites was accompanied by pumice and ash falls (Lp^1) and followed by deposition of a trachyte pumice fall unit (Lp^2). The final stage of collapse saw emplacement of a trachyte ignimbrite (Lp^3). Caldera formation led to interaction of magma with groundwater and early post-caldera eruptions produced a

sequence of trachyte pumice beds and surge units (Lp^4). Post-caldera activity continued with the deposition of a succession of pumice lapilli beds (Lp^5), the oldest of which has been dated at 9150 ± 150 years BP by ^{14}C. The estimated total volume of the caldera pyroclastics in this second stage is 20 km^3 and activity ended by 5650 ± 120 years BP. Scott and Bailey (1986) suggested that inputs of fresh basalt into the root zone of the magmatic system may have initiated each of the pre-caldera pyroclastic events and the subsequent caldera formation.

Scott (1980) calculated a caldera volume of 26.5 km^3 and a syn-caldera erupted magma volume of 11.25 km^3 and suggested that this relationship indicated lateral withdrawal of magma at depth during caldera formation.

Relatively little has been published in detail on the petrology and geochemistry of the eruptives from stages 1 and 2 of Longonot's development, although Scott and Skilling (1999) provided compositional ranges for most units. The pyroclastic deposits apparently mainly comprise comenditic trachytes and pantelleritic trachytes but Clarke et al. (1990) refer to some pumice fragments as phonolites. The same authors reported that decreases in ITE concentrations from bottom to top of some Plinian Lp^5 deposits indicated that the pre-eruptive magma reservoir(s) were compositionally zoned (c.f. Rogers et al., 2004). Data given in Clarke (1987) show that the syn-caldera ignimbrites are also internally differentiated. Similarly, preliminary study at Lancaster University of a Longonot syn-caldera ash flow tuff exposed in the Olkaria Complex shows that it is also compositionally zoned, with ITE enrichment factors ~2.

The Lp^5 unit contains syenite and trachyte lithics, many of which contain sodalite phenocrysts (Clarke et al., 1990). This occurrence, and the recognition of phonolites in some pumice falls, point to an important phase of silica-undersaturated magmatism at Longonot, whose temporal and petrogenetic relationships to the silica-oversaturated rocks need to be clarified.

The final, post-Lp^5, stage of Longonot's history was marked by a shift to predominantly effusive eruptions, the lava sequence stage. Heterogeneously mixed trachyte–hawaiite flows (LMx^1) were followed by eruption of trachytes (Lt^2) to form a cone. Cone growth terminated at 3280 ± 120 years BP, with the eruption of an ash deposit (Lp^8), closely followed by summit collapse to leave a 2 km diameter pit crater.

Subsequent eruption of trachyte (Lt^3) on the volcano's flanks was accompanied by eruption of mixed trachyte–hawaiite flows (Lmx^2) in the pit crater. The youngest flows may be < 1000 years. The total volume of the lava sequence is 18–20 km^3, most of it in the Lt^2 cone-forming trachytes.

The lava groups are dominated by pantelleritic trachytes, each group showing subtle compositional differences to the others. The Lt^2a and Lt^2b magmas were not related to each other but represent the products of crystal fractionation of more mafic, probably hawaiitic, parental magmas. This is consistent with evidence that the mafic and trachytic rocks have similar isotopic compositions (Fig. 7). Differentiation within the trachytes involved 37% crystallization of alkali feldspar-dominated assemblages (Rogers et al., 2004). The proposed differentiation scheme explains adequately the distribution of certain ITE, such as Nb, Zr and Th but there are unresolved problems with the behaviour of others, such as Rb, U, Y and the REE.

Within each group, younger members tend to be more evolved (Fig. 9). In contrast, the Lt^3 lavas reflect mixing between the Lt^2b magma and more mafic material, possibly represented by the LMx^2 lavas. Scott (1982) provided petrographic evidence for a low solubility, CO_2-rich vapour phase coexisting with at least some of the trachyte magmas.

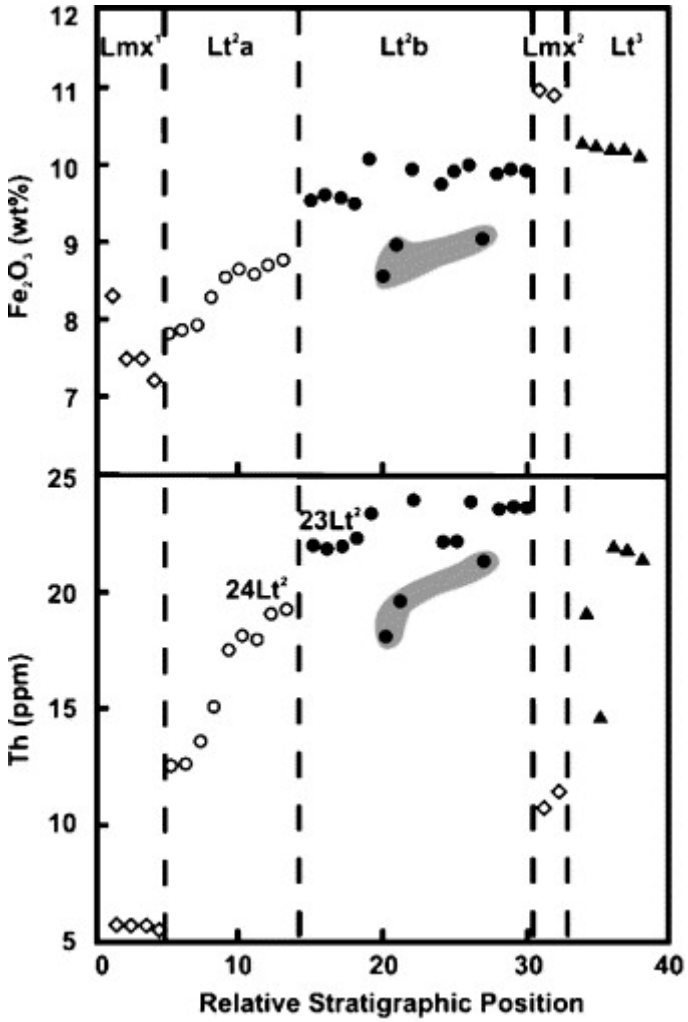

Fig. 9. Variation of Fe_2O_3 and Th abundances with relative stratigraphic height in the Longonot lavas. Note that within the Lt^2a and Lt^2b sequences, both elements generally increase with relative height, i.e. the magmas are becoming more evolved. LMx^1 and LMx^2 represent mixed magma rocks. There is a hiatus between the Lt^2a and Lt^2b fields (from samples 24 to 23) that Rogers et al. (2004) interpreted to mean that the two sequences were derived from slightly different parental magmas. The three samples outlined within the Lt^2b field are anomalous in having compositions more akin to the Lt^2a rocks; see Rogers et al. (2004) for a detailed discussion. Redrawn from Rogers et al. (2004).

The hybrid lavas, LMx^1 and LMx^2, were formed by mixing trachytic magmas with more mafic, probably hawaiitic, magmas. Scott and Bailey (1986) and Rogers et al. (2004) have recorded LMx^1 lavas with Ba ~3950 ppm, suggesting that, as at Menengai, high-Ba magmas were present in the magmatic system but erupted only as mix components. Interestingly, the total range of Pb isotopes in the Longonot trachytes is not consistent with closed system crystal fractionation alone; Rogers et al. (2004) suggested that up to 10% of a typical comendite from the Olkaria complex may have been added to Longonot magmas. This evidence of lateral magma transport is consistent with the suggestion by Scott (1980; see

above) that caldera collapse at Longonot was accompanied by lateral magma withdrawal along regional fractures.

Rogers et al. (2004) used ^{238}U–^{230}Th–^{226}Ra disequilibria to assess rates and timescales of fractional crystallization at Longonot. They interpreted ($^{226}Ra/^{230}Th$) disequilibrium to reflect alkali feldspar fractionation > 8 ka ago in Lt^2a lavas, between 3 and 7 ka in Lt^2b lavas, and < 3 ka in Lt^3 lavas. Fractionation rates from hawaiite to trachyte ($\sim 0.2 \times 10^{-4}$/year) are slower than those within the trachytes (3×10^{-4}/year), prompting Rogers et al. (2004) to propose a two-stage model, whereby hawaiitic magmas initially differentiated in a large, mid-crustal reservoir to produce trachyte melt which ascended into the immediately sub-volcanic reservoir. The Lt^2a magma may have been stored in this upper reservoir for ≥ 2500 years before eruption, without undergoing any further fractionation, whereas evidence from the Lt^2b and Lt^3 lavas suggests that their magmas were erupted as fractionation was proceeding. The reasons for this difference in behaviour have not yet been resolved.

7. Suswa Volcano

The geology of Suswa (1°10′S, 36°20′E) has been described by Johnson (1969) and Skilling (1993) and summarized by Scott and Skilling (1999). Fig. 10 is a schematic representation of the evolution of the inferred magma chamber during all but the latest stages of the volcano's history. Activity began at < 0.4 Ma with the construction of a trachyte lava shield some 28 km in diameter (S1; Fig. 10). After a period of quiescence, activity resumed with the incremental collapse of caldera 1, accompanied by a sequence (S2) of low volume pyroclastic eruptions from vents on an outer ring feeder zone (RFZ; Fig. 10). The succession consists of two trachyte globule ignimbrites (Skilling, 1993), three carbonate–trachyte ignimbrites (Macdonald et al., 1993), eight trachyte pumice lapilli beds and a trachybasaltic ash.

This wide compositional range and the phreatomagmatic and pyroclastic nature of the S2 deposits indicate the complexity of processes during the initial phase of caldera collapse. Magmatic overpressure due to volatile exsolution may have generated the pyroclastic eruptions. Volatile exsolution and/or magma–water interaction may have destabilized the magma chamber (Fig. 10). Alternatively, destabilization may have resulted from introduction of denser trachybasaltic magma into the chamber, either from a zoned chamber beneath Suswa or via lateral propagation from north of the volcano (Skilling, 1993). The trachybasalts have an importance beyond their volumetric abundance, in that they point to the existence of intermediate composition magmas in the Suswa system (c.f. the magmatic inclusions of intermediate composition at Olkaria).

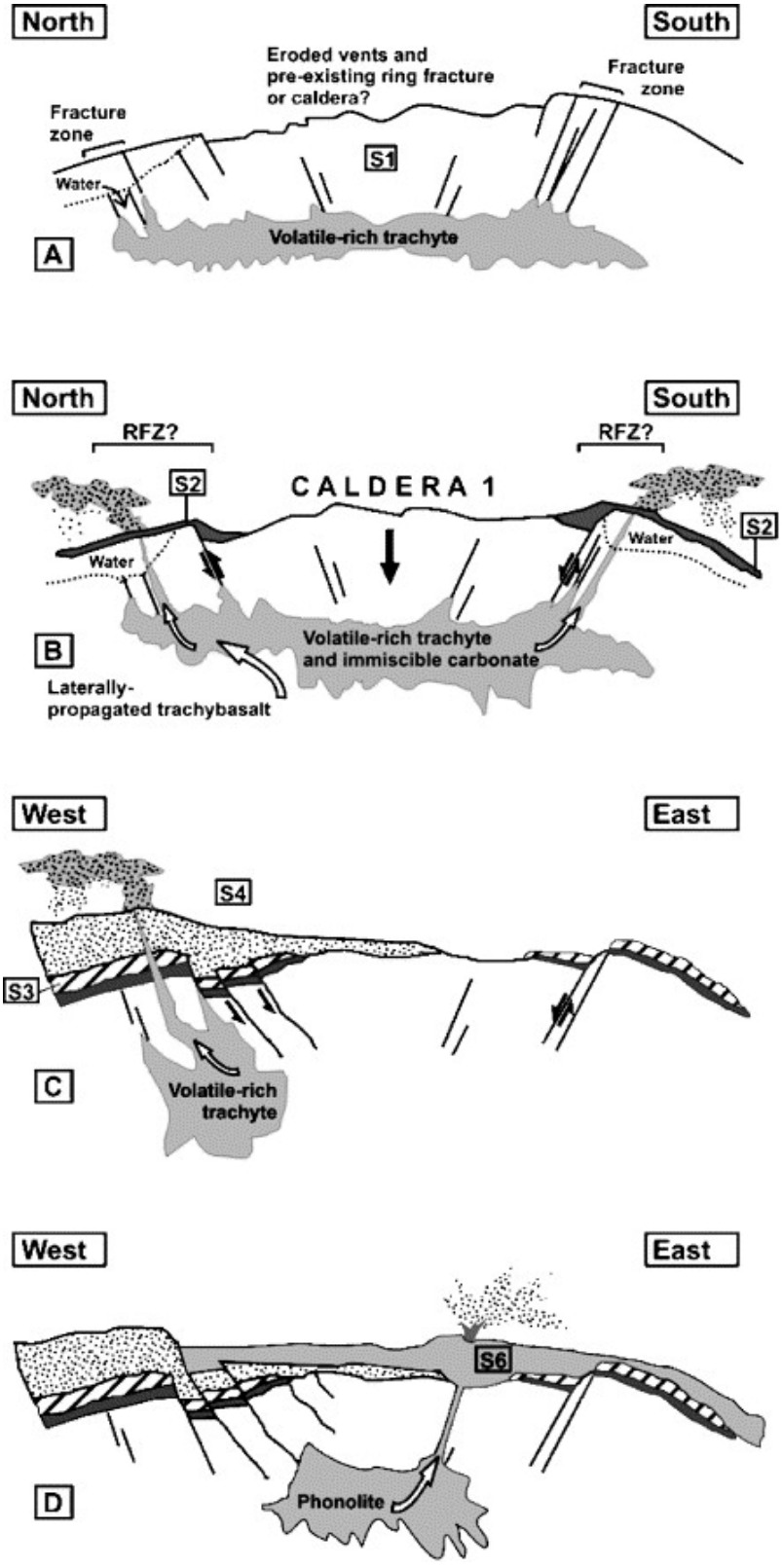

Fig. 10. Schematic representation of the evolution of the Suswa magma chamber from pre-caldera (S1) to early post-caldera (S6) times. The latest stages of development (S7 and S8) are not shown. (A) Development of Ring-Feeder Zone, perhaps by ascent of volatile-rich trachyte. (B) Magma–water interaction and influx of trachybasaltic magma. (C) Eruptions of trachyte in west of caldera. (D) Post-caldera phonolites erupted from vents near the centre of the caldera. Redrawn from Skilling (1993).

With continuing caldera collapse, trachyte agglutinate flows (S3) were erupted from the outer ring feeder zone and trachyte pumice lapilli fall tuffs from the western part of the caldera (S4). Low volume, trachyte lava flows and domes erupted from a fissure zone (S5) signalled the end of caldera 1 formation. The caldera has a minimum volume of ~22 km^3, is ~12 km across and covers an area of ~113 km^2. The estimated volume of syn-caldera deposits is 6 km^3 and Skilling (1993) has proposed magma drainage at depth to explain the discrepancy. Furthermore, Scott and Skilling (1999) demonstrated that the formation of the Suswa caldera was synchronous with that at Longonot, suggesting that caldera formation is a regional rather than local event in this part of the rift, pointing to the potential role of regional tectonics as a controlling mechanism.

Following caldera 1 collapse, phonolite lava flows were erupted from the caldera floor (S6; 0.1 ± 0.01 Ma). Centrally erupted phonolite lavas formed the Ol Doinyo Onyoke cone (S7). Development of a pit crater on the cone was followed by the collapse of caldera 2, both by magma withdrawal at depth. Caldera 2 (5.5 km) is smaller than caldera 1 and is entirely contained within it. Resurgence of the caldera floor to form an "island block" may have been related to regional decompression (Skilling, 1993). The most recent magmatic activity (S8) has been the eruption of phonolite lavas in the ring trench separating the island block from caldera 2 and a single flow on the south flank of the volcano.

No complete geochemical study of Suswa has yet been published. Nash et al. (1969) presented whole-rock and mineral chemical data for 12 lavas, mainly from the younger eruptive episodes, and Scott and Skilling (1999) used whole-rock data from Skilling's (1988) PhD thesis in various trace element plots, mainly to distinguish Suswa from Longonot rocks. Some general features are as follows:

(i) Rocks erupted before the end of caldera 1 formation are trachytes; later rocks are phonolites.

(ii) Whilst the trachytes and phonolites are dominantly peralkaline, metaluminous varieties also occur; for example, the S3 and S7 phonolites.

(iii) There is no correlation between degree of silica undersaturation and the peralkalinity and ITE abundances. Thus, the highest values of AI and ITE are in the trachytes of the WPG unit (S4), and the lowest in the S6 phonolites.

It seems, therefore, that the various units are not directly related to each other but evolved from different parental magmas (Nash et al., 1969). Differentiation within units was dominantly by crystal fractionation (Nash et al., 1969).

In a study of the S2 syn-caldera carbonate–trachyte ignimbrites, Macdonald et al. (1993) showed that the trachyte was metaluminous to peralkaline, and from nepheline- to quartz-normative, in composition. They interpreted compositional variations in the trachyte and carbonatite to indicate that, prior to eruption of the ash flow tuffs, the upper part of the Suswa magma chamber was occupied by a compositionally zoned, carbonated trachyte. After a phase of phenocryst crystallization (dominated by alkali feldspar), a carbonatitic melt exsolved and separated as globules from the silicate. Pressure release related to caldera formation resulted eventually in eruption of the trachytic melt and entrained globules, which are now found as cm-scale banded, silicate–carbonatite tuffs with juvenile pumice fragments having variable proportions of silicate glass to carbonate matrix.

Macdonald et al. (1993) claimed that these rocks provide exceptionally clear evidence of a liquid immiscibility relationship between trachyte and sövite and asked the question, pertinent to peralkaline magmatism in general, as to whether the Suswa case is a unique case, or a uniquely preserved example of a widespread case? Is liquid immiscibility between peralkaline trachyte and carbonatite common, the evidence for it normally being lost because carbonate-rich pyroclasts are easily eroded and/or overlooked?

On the basis of trace element compositions, Scott and Skilling (1999) argued that during or prior to the collapse of caldera 1, there was a small amount of mixing of S2 trachyte magma with O2 comendite magma from Olkaria, the mixing being facilitated by lateral propagation of comendite magma along an N–S tension fracture. This proposal has clear similarities to that by Rogers et al. (2004), noted above, that Olkaria magma has also mixed with Longonot magma.

8. General relevance to peralkaline magmatism

The rocks of the central Kenyan province provide information of general relevance to several aspects of peralkaline magmatism.

(1) Although the caldera volcanoes are dominated by peralkaline trachytes, metaluminous varieties are present at all centres and are normally less evolved than the peralkaline types. The presence of trachybasaltic ashes at Suswa suggests liquid lines of descent leading further back, to the basalts which occur as components of mixed magmas and as intra-centre eruptives. Isotopic evidence (Rogers et al., 2004) makes it likely that the trachytes were derived by fractional crystallization of mafic parental magmas. Despite their paucity at the surface, basalts–trachybasalts have been vitally important as thermal input, especially to the small, rhyolitic systems.

Isotopic evidence seems to indicate that the Olkaria comendites were derived from partial melting of crustal rocks but geochemical problems remain with this scheme. Pantellerites at both Olkaria and in the Eburru Pantellerite Formation may have formed by prolonged fractional crystallization of comenditic magmas. However, pantellerites at Menengai seem to have been generated by fractional crystallization of trachyte and there may well be at least two modes of pantellerite formation recorded in the province.

(2) The development of compositional zonation, as recorded within units ranging in scale from ash falls a few metres thick to ash flow tuffs 30 km^3 in volume, has been ubiquitous in the province. Such zonation has been repeatedly developed through tens of cubic km of magma in times of 10^3–10^4 years. The process may have been facilitated by the low viscosity of the magmas, itself a function of high volatile contents, especially halogens, and high Fe contents.

(3) The centres responded in rather different ways to caldera collapse. At Menengai, loss of volatiles through the chamber resulted in gravitational instability in the chamber which in turn caused convective overturn. This effect may be common in peralkaline systems, where Fe contents increase in more fractionated melts and where the interplay of Fe and volatiles critically determines magma density. The convective overturn after caldera 2 also allowed deeper Ba-rich trachyte magma to rise and mix with the overlying trachyte magma.

In the GOVC, pantelleritic magmatism accompanying caldera formation was replaced by intra-caldera comenditic magmatism. Immediately after collapse of both calderas at Longonot, hawaiite magma mixed with trachyte. Magmatism pre-caldera 1 at Suswa was trachytic in composition; post-caldera and all subsequent activity was phonolitic. The reasons for the different behaviour of these systems presumably include magma composition (including volatile contents), chamber geometry and the effect of local tectonics, particularly in providing new mafic magma into the lower parts of the chamber.

(4) Magma mixing has been a common feature of all the complexes, involving variable combinations of mafic, intermediate, trachytic and rhyolitic magmas. At Suswa and Longonot, a component of the mixing may have been derived from the neighbouring GOVC, the lateral movement of magma having been facilitated by the regional dyke swarm underlying the centres. Such open system behaviour has implications for petrogenetic modelling and for the interpretation of isotopic systematics at each centre.

(5) The Olkaria rhyolites crystallized under conditions of near water saturation. We have no robust evidence regarding the water contents of the trachytes, although the high proportions of pyroclastic rocks at the caldera centres may point to the magmas being hydrous, as well as halogen-rich.

(6) The youthfulness of the peralkaline centres and the high Rb/Sr ratios of the more evolved magma type centres mean that both U-series disequilibria and Rb–Sr isotopic systematics can be employed in determining rates and timescales of, inter alia, pre-eruptive residence times, crystal fractionation processes, and the development of compositional zonation. A start has been made (Black et al., 1997, Heumann and Davies, 2002 and Rogers et al., 2004) but the province holds considerable potential for further such work.

(7) Variations in Zr concentration with time at Menengai (Fig. 11) clearly make the point that in all the centres of the central Kenya peralkaline province, the greatest compositional diversity is usually found in the pyroclastic rocks. Sampling of lavas alone could give a very biased view of the total compositional range. The complex geochemical evolution which characterises peralkaline volcanoes is revealed only by detailed sampling of all eruptive units, tied to a firm stratigraphic framework.

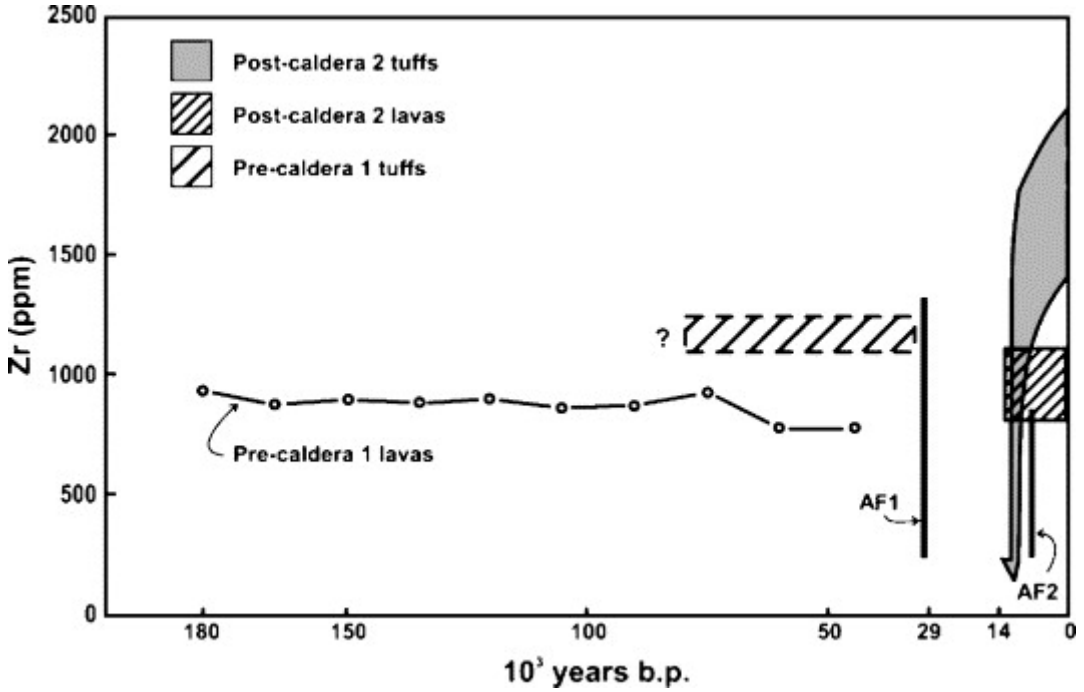

Fig. 11. Zr concentrations plotted against time for the eruptive products of Menengai. The compositional diversity within the pyroclastic deposits (pre-caldera tuffs, ash flows AF1 and AF2, and post-caldera-tuffs) is considerably greater than in the lavas.

Acknowledgements

RM would like to thank the National Environment Research Council (UK) for support through research grants and studentships. Philip Leat, Gregor Markl and John White provided helpful manuscript reviews and editorial comment

References

Bailey, 1974 D.K. Bailey, Experimental petrology relating to oversaturated peralkaline volcanic rocks: a review, *Bull. Volcanol.* **38** (1974), pp. 635–652.

Bailey and Macdonald, 1975 D.K. Bailey and R. Macdonald, Fluorine and chlorine in peralkaline liquids and the need for magma generation in an open system, *Mineral. Mag.* **40** (1975), pp. 405–414.

Bailey and Macdonald, 1987 D.K. Bailey and R. Macdonald, Dry peralkaline felsic liquids and carbon dioxide flux through the Kenya rift zone. In: B. Mysen, Editor, *Magmatic Processes: Physiochemical Principles*, *Geochem. Soc. Spec. Publ.* **vol. 1** (1987), pp. 91–105.

Black et al., 1997 S. Black, R. Macdonald and M.R. Kelly, Crustal origin for peralkaline rhyolites from Kenya: evidence from U-series disequilibria and Th isotopes, *J. Petrol.* **38** (1997), pp. 277–297.

Clarke, 1987 Clarke, M.C.G., 1987. Compilation and interpretation of rock geochemical data for the Longonot Volcano and the Greater Olkaria Volcanic Complex. British Geological Survey Report Genken/5/.

Clarke et al., 1990 M.C.G. Clarke, D.G. Woodhall, D. Allen and G. Darling, Geological, volcanological and hydrological controls on the occurrence of geothermal activity in the area surrounding Lake Naivasha, Kenya, *British Geological Survey and Kenyan Ministry of Energy*, Derry and Sons Ltd, Nottingham (1990) 138 pp..

Davies and Macdonald, 1987 G.R. Davies and R. Macdonald, Crustal influences in the petrogenesis of the Naivasha basalt–comendite complex: combined trace element and Sr–Nd–Pb isotope constraints, *J. Petrol.* **28** (1987), pp. 1009–1031.

Heumann and Davies, 2002 A. Heumann and G.R. Davies, U–Th disequilibrium and Rb–Sr age constraints on the magmatic evolution of peralkaline rhyolites from Kenya, *J. Petrol.* **43** (2002), pp. 557–577.

Johnson, 1969 R.W. Johnson, Volcanic geology of Mount Suswa, *Philos. Trans. R. Soc. Lond., A* **265** (1969), pp. 383–412.

Leat, 1984 P.T. Leat, Geological evolution of the trachytic caldera volcano Menengai, Kenya Rift Valley, *J. Geol. Soc. (Lond.)* **141** (1984), pp. 1057–1069.

Leat, 1985 P.T. Leat, Facies variations in peralkaline ash-flow tuffs from the Kenya Rift Valley, *Geol. Mag.* **122** (1985), pp. 139–150.

Leat et al., 1984 P.T. Leat, R. Macdonald and R.L. Smith, Geochemical evolution of the Menengai caldera volcano, Kenya, *J. Geophys. Res.* **89** (1984), pp. 8571–8592.

Macdonald, 1974 R. Macdonald, Nomenclature and petrochemistry of the peralkaline oversaturated extrusive rocks, *Bull. Volcanol.* **38** (1974), pp. 498–516.

Macdonald, 1987 R. Macdonald, Quaternary peralkaline silicic rocks and caldera volcanoes of Kenya. In: J.G. Fitton and B.G.J. Upton, Editors, *Alkaline Igneous Rocks*, *Geol. Soc. London Spec. Publ.* **vol. 30** (1987), pp. 313–333.

Macdonald et al., 1987 R. Macdonald, G.R. Davies, C.M. Bliss, P.T. Leat, D.K. Bailey and R.L. Smith, Geochemistry of high-silica peralkaline rhyolites, Naivasha, Kenya Rift Valley, *J. Petrol.* **28** (1987), pp. 979–1008.

Macdonald et al., 1993 R. Macdonald, B.A. Kjarsgaard, I.P. Skilling, G.R. Davies, D.L. Hamilton and S. Black, Liquid immiscibility between trachyte and carbonate in ash flow tuffs from Kenya, *Contrib. Mineral. Petrol.* **114** (1993), pp. 276–287.

Macdonald et al., 1994 R. Macdonald, J.M. Navarro, B.G.J. Upton and G.R. Davies, Strong compositional variation in peralkaline magma: Menengai, Kenya Rift Valley, *J. Volcanol. Geotherm. Res.* **60** (1994), pp. 301–325.

Mahood, 1984 G.A. Mahood, Pyroclastic rocks and calderas associated with strongly peralkaline magmatism, *J. Geophys. Res.* **89** (1984), pp. 8540–8552.

Marshall and Macdonald, 1998 A.S. Marshall and R. Macdonald, Evolution of magmatic plumbing systems, Naivasha, Kenyan Rift Valley (abs.), *IAVCEI Intern. Geol. Congr., Cape Town, July, 1998* (1998), p. 40.

Mechie et al., 1997 J. Mechie, G.R. Keller, C. Prodehl, M.A. Khan and S.J. Gaciri, A model for the structure, composition and evolution of the Kenya rift, *Tectonophysics* **278** (1997), pp. 95–119.

Mooney and Christensen, 1994 W.D. Mooney and N.I. Christensen, Composition of the crust beneath the Kenya rift, *Tectonophysics* **236** (1994), pp. 391–408.

Nash et al., 1969 W.P. Nash, I.S.E. Carmichael and R.W. Johnson, The mineralogy and petrology of Mount Suswa, Kenya, *J. Petrol.* **10** (1969), pp. 409–439.

Novak and Mahood, 1986 S.W. Novak and G.A. Mahood, Rise and fall of a basalt–trachyte–rhyolite magma system at the Kane Springs Wash Caldera, Nevada, *Contrib. Mineral. Petrol.* **94** (1986), pp. 352–373.

Ren et al., 2006-this volume M. Ren, E.Y. Anthony, P.A. Omenda, J.C. White, R. Macdonald and D.K. Bailey, Application of the QUILF thermobarometer to the peralkaline trachytes and pantellerites of the Eburru volcanic complex, East African Rift, Kenya. Lithos (2006).

Rogers et al., 2004 N.W. Rogers, P.J. Evans, S. Blake, S.C. Scott and C.J. Hawkesworth, Rates and timescales of fractional crystallization from ^{238}U–^{230}Th–^{226}Ra disequilibria in trachyte lavas from Longonot volcano, Kenya, *J. Petrol.* **45** (2004), pp. 1747–1776.

Scaillet and Macdonald, 2001 B. Scaillet and R. Macdonald, Phase relations of peralkaline silicic magmas and petrogenetic implications, *J. Petrol.* **42** (2001), pp. 825–845.

Scaillet and Macdonald, 2003 B. Scaillet and R. Macdonald, Experimental constraints on the relationships between peralkaline rhyolites of the Kenya rift valley, *J. Petrol.* **44** (2003), pp. 1867–1894.

Scott, 1980 S.C. Scott, The geology of Longonot volcano, Central Kenya: a question of volumes, *Philos. Trans. R. Soc. Lond., A* **296** (1980), pp. 437–465.

Scott, 1982 S.C. Scott, Evidence from Longonot volcano, Central Kenya, lending further support to the argument for a coexisting CO_2 rich vapour in peralkaline magma, *Geol. Mag.* **119** (1982), pp. 215–217.

Scott and Bailey, 1986 S.C. Scott and D.K. Bailey, Coeruption of contrasting magmas and temporal variations in magma chemistry at Longonot volcano, Central Kenya, *Bull. Volcanol.* **47** (1986), pp. 849–873.

Scott and Skilling, 1999 S.C. Scott and I.P. Skilling, The role of tephrachronology in recognising synchronous caldera-forming events at the Quaternary volcanoes Longonot and Suswa, south Kenya Rift. In: C.R. Firth and W.J. McGuire, Editors, *Volcanoes in the Quaternary*, *Spec. Publ. Geol. Soc. London* **vol. 161** (1999), pp. 47–67.

Skilling, 1988 Skilling, I.P., 1988. The geological evolution of Suswa volcano. Kenya. PhD thesis, University of Lancaster.

Skilling, 1993 I.P. Skilling, Incremental caldera collapse of Suswa volcano, Gregory Rift Valley, Kenya, *J. Geol. Soc. (Lond.)* **150** (1993), pp. 885–896.

Smith, 1994 M. Smith, Stratigraphic and structural constraints on mechanisms of active rifting in the Gregory Rift, Kenya, *Tectonophysics* **236** (1994), pp. 3–22.

Swain, 1992 C.J. Swain, The Kenya rift axial gravity high: a reinterpretation, *Tectonophysics* **204** (1992), pp. 59–70.

Wilding et al., 1993 M.C. Wilding, R. Macdonald, J.E. Davies and A.E. Fallick, Volatile characteristics of peralkaline rhyolites from Kenya: an ion microprobe, infrared spectroscopic and hydrogen isotope study, *Contrib. Mineral. Petrol.* **114** (1993), pp. 264–275